academicJournals

Vol. 5(1), pp. 1-10, April 2014
DOI 10.5897/JCECT2013.0001
Article Number: 06E330D44286
ISSN 2141-2634

http://www.academicjournals.org/JCECT

Journal of Civil Engineering and Construction Technology

Full Length Research Paper

Effects of bridge length and span variations in curved integral abutment bridges

Jhunyawhatt Thaanasarttayawibul[1], Amde M. Amde[2] and Andreas Paraschos[3]*

[1]TCC Land Company Limited, Thailand.
[2]Department of Civil and Environmental Engineering United States, University of Maryland, United States.
[3]New York City Department of Transportation/Division of Bridges United States.

Received 2 July, 2013; Accepted 3 January, 2014

This paper presents the results of a parametric study that focused on the effects of bridge length and span variations on the maximum stress intensity (stress concentration) in the piles of horizontally-curved steel I-girder integral abutment bridges. Over 1,700 three-dimensional nonlinear finite element models with bridge lengths up to 365 m (1200 ft) were analyzed as part of this study. The results indicate that the stress concentration in the piles increases with increasing bridge length and reaches its maximum value at a certain bridge length. Beyond that bridge length, pile stress concentration decreases despite the fact that bridge length continues to increase. This represents a difference in behavior compared to straight integral abutment bridges where the pile stress concentration always increases with increasing bridge length. The study also indicates that curved integral abutment bridges of smaller radius have a larger pile stress intensity reduction due to increased number of spans compared to curved integral abutment bridges of larger radius.

Key words: Integral abutment bridges, curved bridges, finite element modeling, thermal loads.

INTRODUCTION

Straight integral abutment bridges were studied by many researchers (Jorgenson, 1983; Yang et al., 1985; Greimann et al., 1986, 1987, 1988; Amde et al., 1988, 1997; Griton et al., 1991; Lawver et al., 2000; Paraschos and Amde, 2010). They concluded that thermal gradient had a relatively small effect on the movements of the abutments and piers of bridges up to 91 m (300 ft) in length. Its effect on bridges longer than 91 m (300 ft) in length might be significant. Skewed integral abutment bridges were studied by Greimann and Amde (Greimann et al., 1983) and Haj-Najib (Haj-Najib, 2002). They concluded that for bridges with skew up to 10° and an anticipated movement at each abutment of ± 1 cm (± 0.375 in) shall be treated as straight integral abutment bridges. For integral abutments, as their length and skew increases, temperature-induced stresses become more critical to the piling load capacities. This paper is focused on horizontally curved steel I-girder integral abutment bridges (hereafter referred to as curved IAB's) with a degree of curvature ranging from 0 to 172°

*Corresponding author. E-mail: andreas_paraschos@yahoo.com.

Table 1. Material properties and loading.

Materials	Value
Concrete	
Slab (thickness)	7 in.
Abutment (width × height)	3 ft × 7 ft 7 in.
Steel	
Girders	W30 × 132
Cross-bracings	L6 × 6 × 1
Piles	HP10 × 42
Material properties	
Concrete	
Modulus of elasticity	4 ksi
Weight	145 lb/ft^3
Coefficient of thermal expansion	6 × 10^{-6} in./in./°F
Steel	
Modulus of elasticity	36 ksi
Weight	490 lb/ft^3
Coefficient of thermal expansion	6.5 × 10^{-6} in./in./°F
Soil	Figure 2.
Loads	
Dead load	Self weight of bridge structure
Live load	HS20-44 lane loading
Thermal load	ΔT_{slab} = 90° F and $\Delta T_{the\ rest}$ = 60° F
	ΔT_{slab} = 120° F and $\Delta T_{the\ rest}$ = 90° F

and bridge length up to 365 m (1200 ft). The results of the study are used to make recommendations on the design and construction of horizontally curved steel I-girder IAB's.

METHODOLOGY

Over 1,700 three-dimensional finite element models were developed as part of a parametric study to investigate the effects of an increasing bridge length ranging from 15 (50) to 365 m (1200 ft) and the effects of span length variation on the maximum stress intensity developed in the piles of curved steel I-girder IAB's. The research study was conducted using the temperature ranges for moderate climate as per AASHTO Specifications. Two temperature load cases were studied in this analysis. The first temperature load case was a temperature differential of 90° F for concrete slab and the top 3.5 inches of both abutments and the temperature differential of 60° F for the rest of the bridge structures which were steel girders, abutments and piles (ΔT_{slab} of 90° F and $\Delta T_{the\ rest}$ of 60°F). The second temperature load case was a temperature differential of 120° F for concrete slab and the top 3.5 inches of both abutments and the temperature differential of 90° F for the rest of the bridge structures which were steel girders, abutments and piles (ΔT_{slab} of 120° F and $\Delta T_{the\ rest}$ of 90° F). The temperature distribution was varying uniformly in both cases. The models were analyzed using a finite element software, ANSYS, by ANSYS, Inc. The finite element models included the entire integral abutment bridge structure; superstructure, substructure and foundations. They included elements to simulate the nonlinear soil-structure and soil-pile interaction and selected soil profiles.

Material properties and loadings are shown in Table 1. Elements used in the three-dimensional model are listed in Table 2. The typical section of the bridge superstructure is shown in Figure 1. Figure 2 shows graphical representations for the four soil profiles. Table 3 shows the curved IAB parameters used in this study while Figure 3 presents a plot of various radii for the case of a 365 m (1200 ft) long IAB. End-bearing piles were used throughout this study. A sample model used in the analysis before and after applying forces is shown in Figure 4.

RESULTS

Effect of bridge length variation

Figures 5 to 10 indicate that the maximum stress intensity in the piles of curved IAB's increases as the bridge length is increased. The maximum stress intensity in the piles will reach its highest value at a certain bridge length. Beyond that bridge length, pile stress concentration

Table 2. Elements in model.

Element	Description	Degree of Freedom	Model
SHELL 43	a 4-node plastic shell	6 DOFs at each node: translations and rotations	Slabs, girders and piles
BEAM 4	3D elastic beam	6 DOFs at each node: translations and rotations	Cross bracings
SOLID 45	an 8-node plastic solid element	3 DOFs at each node: translations	Abutments
MPC184	Multipoint constraint elements with rigid beam option	6 DOFs at each node: translations and rotations	Connect all elements together
COMBIN39	Nonlinear spring	3 DOFs at each node: translations	Soil

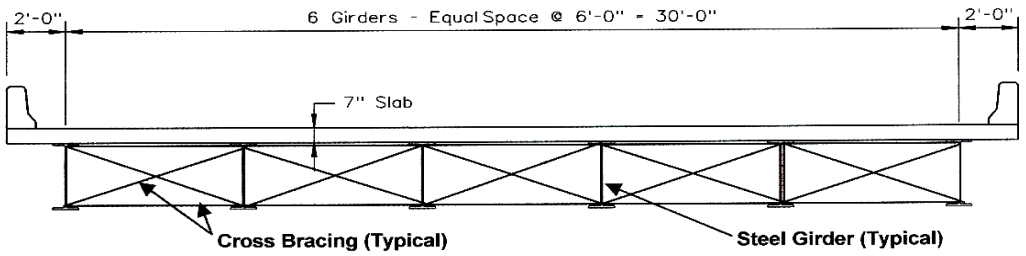

Figure 1. Typical section of the bridge superstructure.

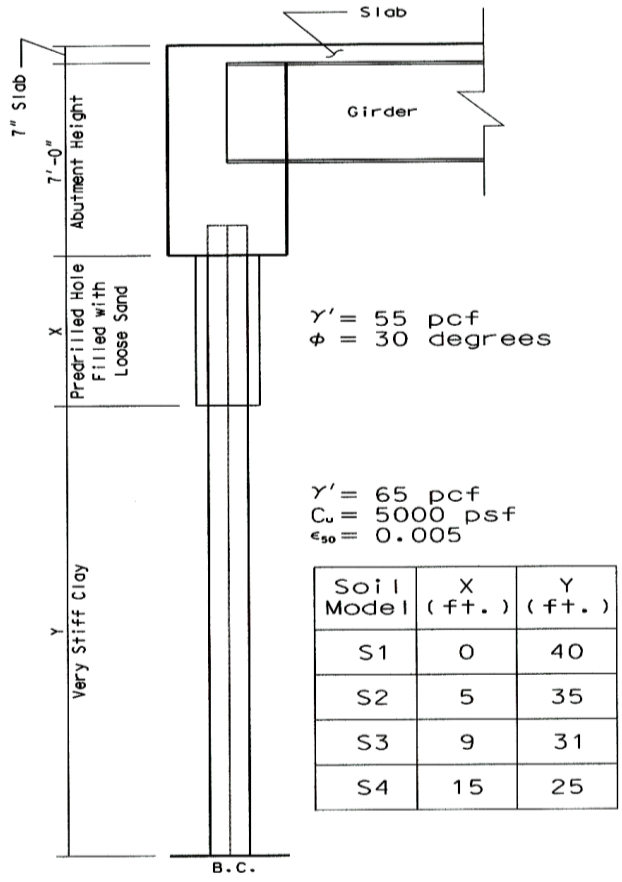

Soil Model	X (ft.)	Y (ft.)
S1	0	40
S2	5	35
S3	9	31
S4	15	25

Figure 2. Soil properties and layout for the different soil profile models.

decreases despite the fact that bridge length continues to increase up to a bridge length of 365 m (1200 ft). This represents a difference in behavior compared to straight integral abutment bridges where the pile stress concentration always increases with increasing bridge length. Figures 5 to 7 also indicate that the maximum stress intensity in the piles of curved IAB's with a 122 m (400 ft) radius and 15 m (50 ft) spans is almost constant for bridge lengths from 244 (800) to 365 m (1200 ft). The lengths of curved IAB's with the highest stress intensity in the piles from Figures 5 to 10 are plotted in Figure 11. The maximum stress intensity in the piles in very stiff clay soil profile (no predrilled holes) of curved IAB's of all radii starts to increase from a 15 m (50 ft) bridge length until it reaches its highest value at the bridge length indicated in Figure 11 (solid line). Beyond that bridge length, the highest pile stress intensity value will start decreasing as the bridge length is increased (dashed and dotted lines). For piles in predrilled holes, the maximum stress intensity in the piles of curved IAB's of all radii starts to increase from a 15 m (50 ft) bridge length until it reaches its highest value at the bridge length indicated in Figure 11 (dashed line). Beyond that bridge length, the highest pile stress intensity value will start decreasing even though bridge length keeps increasing (dotted line). Figure 11 also indicates that the highest stress intensity value in the piles of curved IAB's with radii of 122 m (400 ft) and infinity (straight IAB's) is at the same bridge length [a 122 m (400 ft) length for a 122 m (400 ft) radius, and a 365 m(1200 ft) length for an infinite radius] for piles in all soil profile types. The introduction of predrilled holes results

Table 3. Information of curved integral abutment bridges.

Span length (ft)	Number of spans	Bridge length (ft)	Degree of curvature (degrees) for radius					
			400 ft	600 ft	800 ft	1200 ft	2400 ft	Infinity
50	1	50	7.162	4.775	3.581	2.387	1.194	0
	2	100	14.324	9.549	7.162	4.774	2.387	0
	3	150	21.486	14.324	10.743	7.162	3.581	0
	4	200	28.648	19.099	14.324	9.548	4.775	0
	6	300	42.972	28.648	21.486	14.322	7.162	0
	8	400	57.296	38.197	28.648	19.096	9.549	0
	12	600	85.944	57.296	42.972	28.644	14.324	0
	16	800	114.592	76.394	57.296	38.192	19.099	0
	20	1000	143.239	95.493	71.620	47.746	23.873	0
	24	1200	171.888	114.592	85.944	57.288	28.648	0
100	1	100	14.324	9.549	7.162	4.774	2.387	0
	2	200	28.648	19.099	14.324	9.548	4.775	0
	3	300	42.972	28.648	21.486	14.322	7.162	0
	4	400	57.296	38.197	28.648	19.096	9.549	0
	6	600	85.944	57.296	42.972	28.644	14.324	0
	8	800	114.592	76.394	57.296	38.192	19.099	0
	10	1000	143.239	95.493	71.620	47.746	23.873	0
	12	1200	171.888	114.592	85.944	57.288	28.648	0

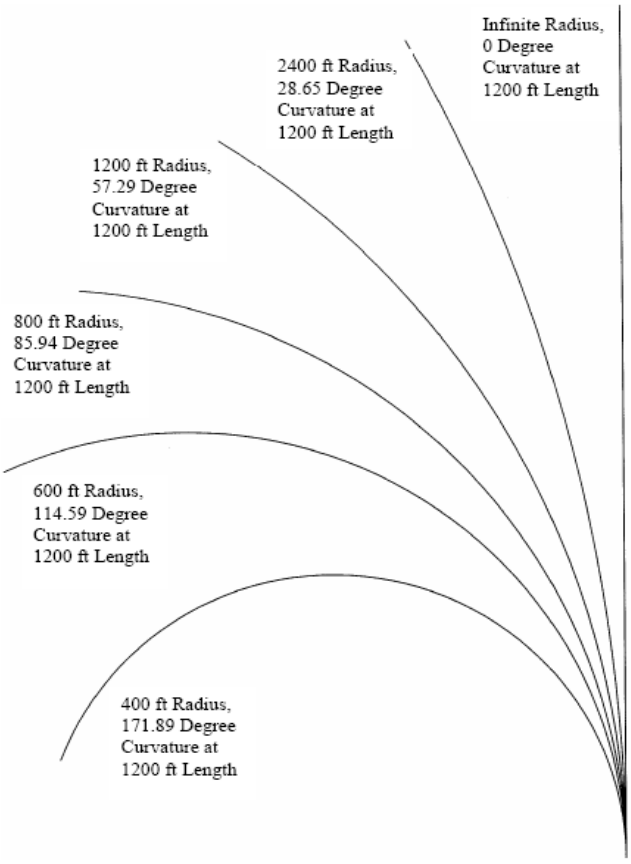

Figure 3. 365 m (1200 ft) long curved integral abutment bridges on varying radii.

Figure 4. Undeformed and deformed shape of a curved integral abutment bridge with 400 ft radius and 4 to 50 ft spans with 28.65° of curvature with piles in very stiff clay soil profile with 9 ft deep predrilled holes filled with loose sand. The bridge is subjected to a thermal load of ΔT_{slab} of 120° F and $\Delta T_{the\ rest}$ of 90° F. A deflection scale factor of 40 is used to enlarge the displacement of the bridge structure.

in the highest stress intensity value in the piles of curved IAB's with radii of 183 (600), 244 (800), 365 (1200) and 731 m (2400 ft) occurring at 61 m (200 ft) longer bridge length compared to the highest stress intensity value in the piles without predrilled holes.

For piles in very stiff clay soil profile, curved IAB's of all radii have approximately the same maximum stress intensity value in the piles at the same bridge length for bridge lengths up to 91 m (300 ft). Beyond the 91 m (300 ft) length, curved IAB's with a smaller radius, for the most part, have a maximum stress intensity in the piles less than that of curved IAB's with a larger radius as the bridge length is increased. For piles in predrilled holes,

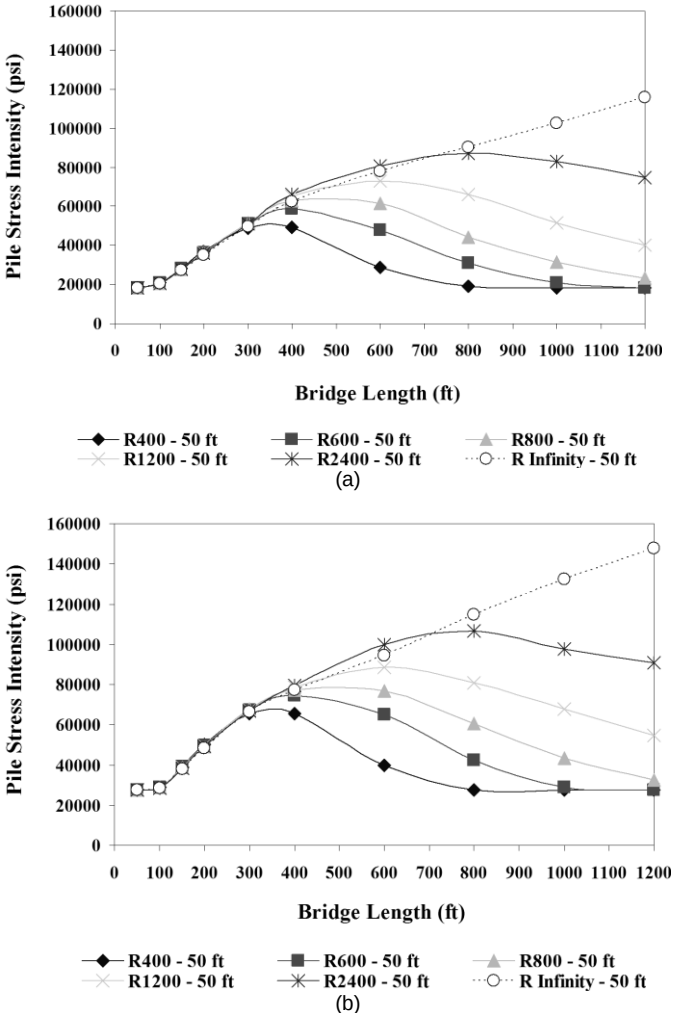

Figure 5. Maximum stress intensity in end-bearing piles in very stiff clay soil profile of bridges with 15 m (50 ft) spans. a) ΔT_{slab} = 90° F, $\Delta T_{the\ rest}$ = 60° F; b) ΔT_{slab} = 120° F, $\Delta T_{the\ rest}$ = 90° F.

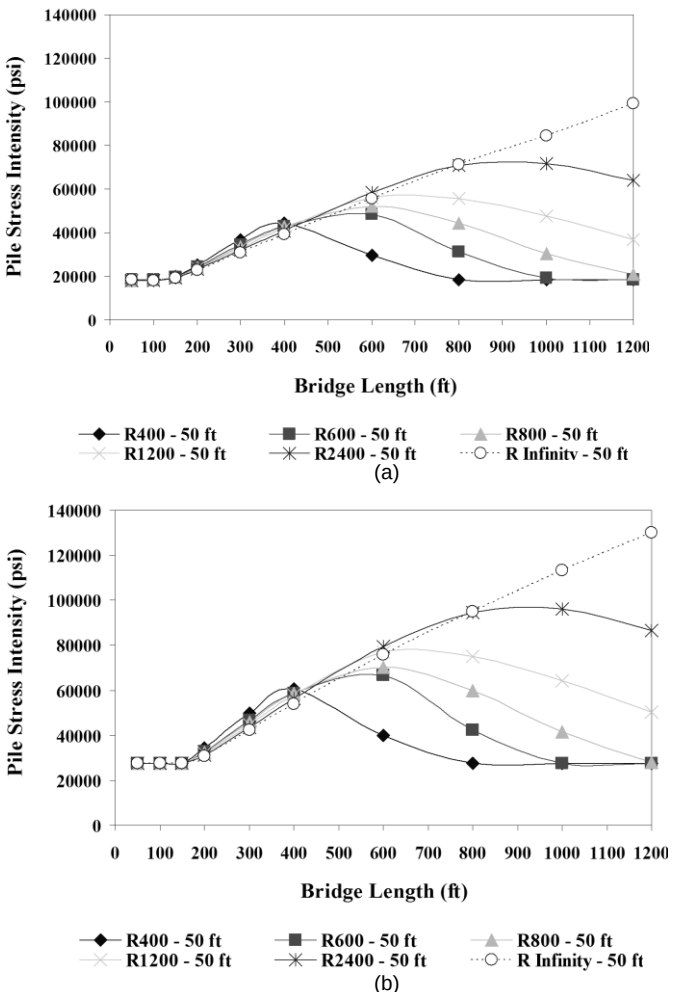

Figure 6. Maximum stress intensity in end-bearing piles in 1.5 m (5 ft) deep predrilled holes of bridges with 15 m (50 ft) spans. a) ΔT_{slab} = 90° F, $\Delta T_{the\ rest}$ = 60° F; b) ΔT_{slab} = 120° F, $\Delta T_{the\ rest}$ = 90° F.

curved IAB's with a larger radius have a maximum stress intensity in the piles less than that of curved IAB's with a smaller radius for bridge lengths up to 122 m (400 ft). Beyond the 122 m (400 ft) length, curved IAB's with a smaller radius, for the most part, have a maximum stress intensity in the piles less than that of curved IAB's with a larger radius as the bridge length is increased. For curved IAB's with 30 m (100 ft) spans and with piles in predrilled holes, curved IAB's with double spans [bridge length of 61 m (200 ft)] can reduce the maximum stress intensity in the piles when compared with single span bridges [bridge length of 30 m (100 ft)]. The pile stress intensity reduction is in the range of 9.5 to 22% for ΔT 90° F and is in the range of 2.6 to 16.4% for ΔT 120° F as indicated in Figure 12. Figure 12 indicates that for piles in predrilled holes, curved IAB's with a smaller radius have a pile stress intensity reduction less than that of curved IAB's with a larger radius when comparing curved IAB's with multi-span bridges consisting of two spans 61 m (200 feet) each with single span bridges [bridge length of 30 m (100 ft)]. It is shown that a temperature increase results in a lower pile stress intensity reduction. Curved IAB's subjected to a temperature load of 120° F have a pile stress intensity reduction less than that of curved IAB's subjected to a temperature load of 90° F.

It is also shown that 2.7 m (9 ft) deep predrilled holes filled with loose sand produce a higher reduction in the pile stress intensity compared to 1.5 m (5 ft) deep predrilled holes filled with loose sand. However, for predrilled holes deeper than 2.7 m (9 ft), the rate of reduction is significantly reduced, which results in only marginal reductions in pile stress intensity.

Effect of span length variation

For piles in very stiff clay soil profile as shown in Figure

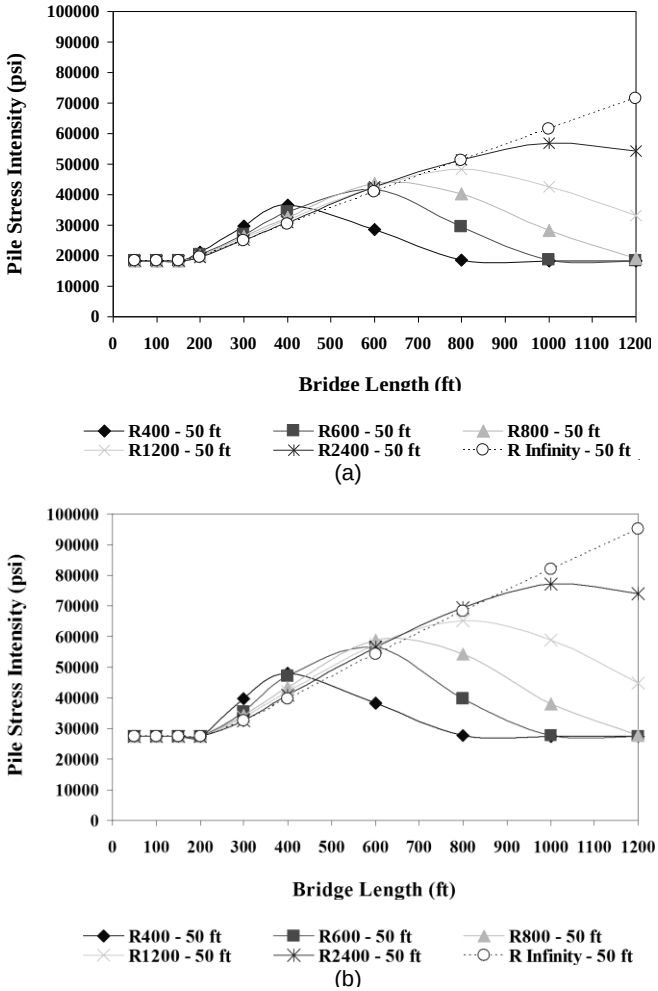

Figure 7. Maximum stress intensity in end-bearing piles in 2.7 m (9 ft) deep predrilled holes of bridges with 15 m (50 ft) spans. a) ΔT_{slab} = 90° F, $\Delta T_{the\ rest}$ = 60° F; b) ΔT_{slab} = 120° F, $\Delta T_{the\ rest}$ = 90° F.

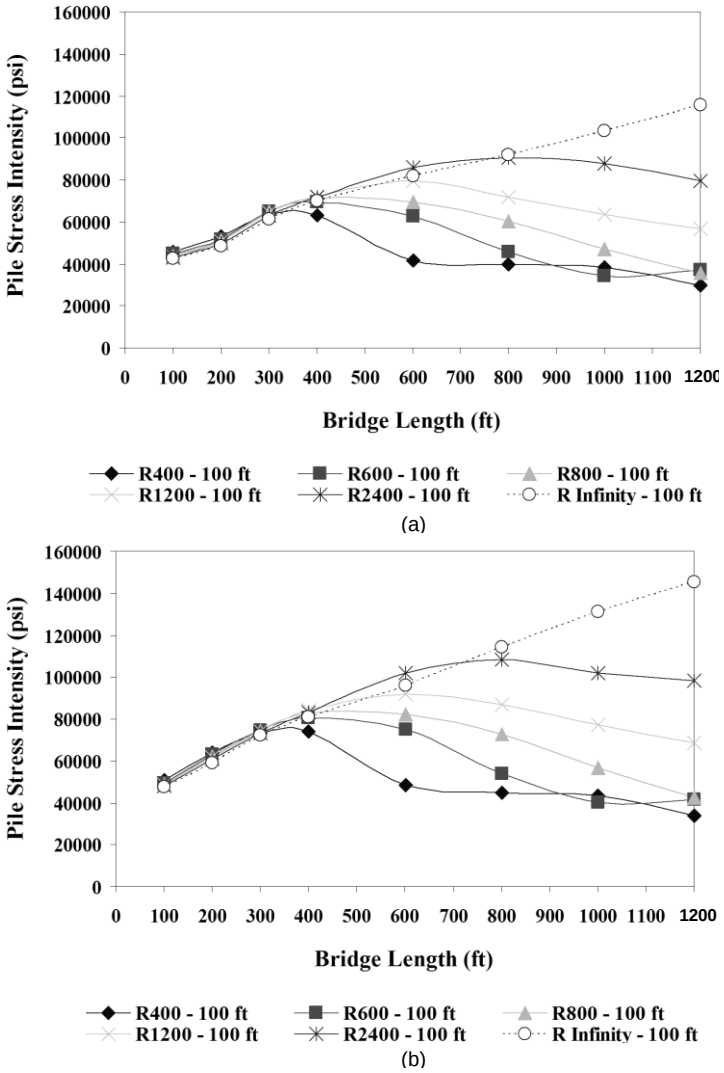

Figure 8. Maximum stress intensity in end-bearing piles in very stiff clay soil profile of bridges with 30 m (100 ft) spans. a) ΔT_{slab} = 90° F, $\Delta T_{the\ rest}$ = 60° F; b) ΔT_{slab} = 120° F, $\Delta T_{the\ rest}$ = 90° F.

13, the highest pile stress intensity reduction value due to the increase in the number of spans of curved IAB's of all radii is between 52.2 and 54.2% for ΔT 90° F and between 40.5 and 42.6% for ΔT 120° F at a 30 m (100 ft) bridge length. It decreases to its lowest value at a certain bridge length. After it reaches its lowest value, almost all pile stress intensity reduction rates start increasing and continue to increase as the bridge length is increased to 365 m (1200 ft). Except curved IAB's with a 122 m (400 ft) radius, after the pile stress intensity reduction rate reaches its lowest value at the bridge length between 91 to 122 m (300 to 400 ft), then the pile stress intensity reduction rate starts to increase as the bridge length is increased until it has the highest value at a 305 m (1000 ft) length and beyond a 305 m (1000 ft) length the pile stress intensity reduction rate decreases again as the bridge length is increased to 365 m (1200 ft). For piles in 2.7 m (9 ft) deep predrilled holes filled with loose sand as shown in Figure 14, the highest pile stress intensity reduction value due to the increase in the number of spans of curved IAB's of all radii is between 61.8 and 64.7% for ΔT 90° F and between 45.6 and 50.8% for ΔT 120° F at a 30 m (100 ft) bridge length. It decreases to its lowest value at a certain bridge length. After they reach their lowest value, some of the pile stress intensity reduction rates showed an increase as the bridge length is increased to 365 m (1200 ft).

Figure 15 indicates that the pile stress intensity reduction due to the increase in the number of spans of curved IAB's with piles in predrilled holes is greater than that of curved IAB's with piles without predrilled holes. It is shown that piles in 2.7 m (9 ft) deep predrilled holes filled with loose sand have a significant reduction in the pile stress intensity when compared with piles in 1.5 m (5 ft) deep predrilled holes filled with loose sand. The depth

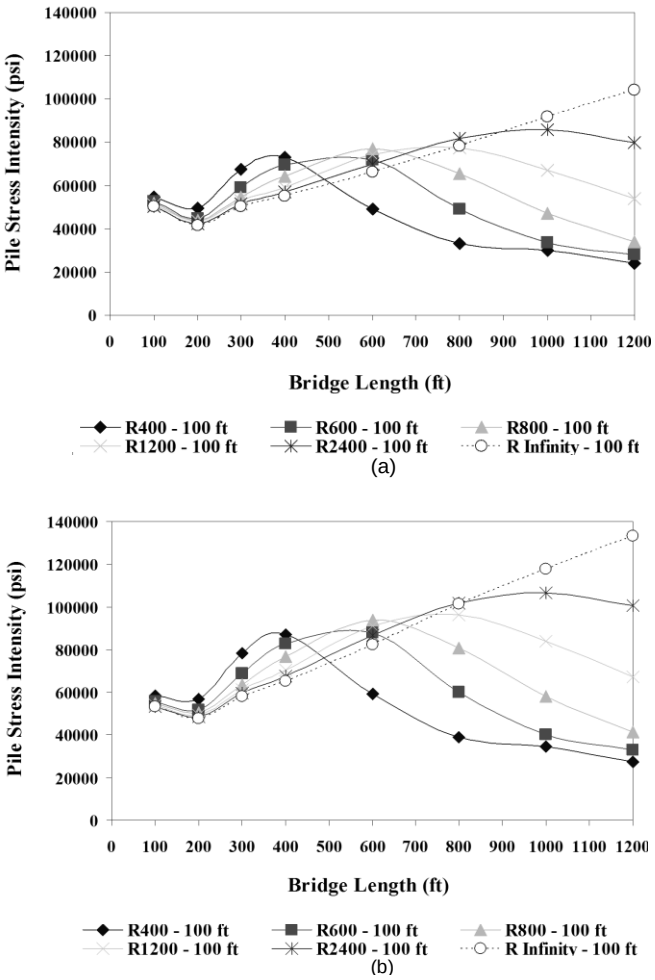

Figure 9. Maximum stress intensity in end-bearing piles in 1.5 m (5 ft) deep predrilled holes of bridges with 30 m (100 ft) spans. a) ΔT_{slab} = 90° F, $\Delta T_{the\ rest}$ = 60° F; b) ΔT_{slab} = 120° F, $\Delta T_{the\ rest}$ = 90° F.

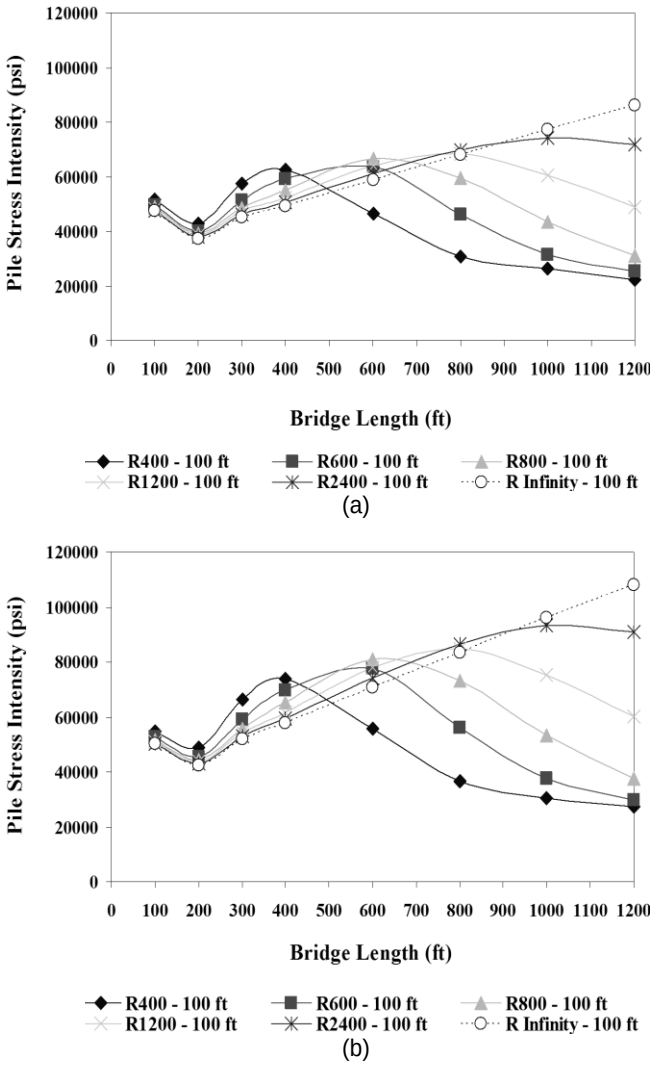

Figure 10. Maximum stress intensity in end-bearing piles in 2.7 m (9 ft) deep predrilled holes of bridges with 30 m (100 ft) spans. a) ΔT_{slab} = 90° F, $\Delta T_{the\ rest}$ = 60° F; b) ΔT_{slab} = 120° F, $\Delta T_{the\ rest}$ = 90° F.

increase of predrilled holes deeper than 2.7 m (9 ft) will further reduce the stress intensity in the piles, but the rate of reduction is much smaller than that of 2.7 m (9 ft) deep predrilled holes. Figures 13 and 15 indicate that curved IAB's with a smaller radius, for the most part, have a pile stress intensity reduction due to the increase in the number of spans greater than that of curved IAB's with a larger radius. The difference in the pile stress intensity reduction due to the increase in the number of spans between curved IAB's with different radii is smaller when predrilled holes are used for the piles compared to the piles with no predrilled holes as shown in Figure 15. In addition, larger temperature increases result in lower pile stress intensity reduction compared to smaller temperature increases.

DISCUSSION

(1) The radius of curvature of IAB's is an important parameter in their design and construction. Curved IAB's with a larger radius and with piles in very stiff clay soil profile have a maximum stress intensity (stress concentration) in the piles less than that of curved IAB's with a smaller radius for bridge lengths up to 91 m (300 ft). It is the same for curved IAB's with piles in predrilled holes for bridge lengths up to 122 m (400 ft). Beyond those bridge lengths, curved IAB's with a smaller radius and with piles in all soil profile types, for the most part, have a maximum stress intensity in the piles less than that of curved IAB's with a larger radius as the bridge length is increased to 365 m (1200 ft).

(2) For straight IAB's, the maximum stress intensity (stress concentration) in the piles increases as the bridge length is increased. In the case of curved IAB's, the maximum stress intensity in the piles begins to increase

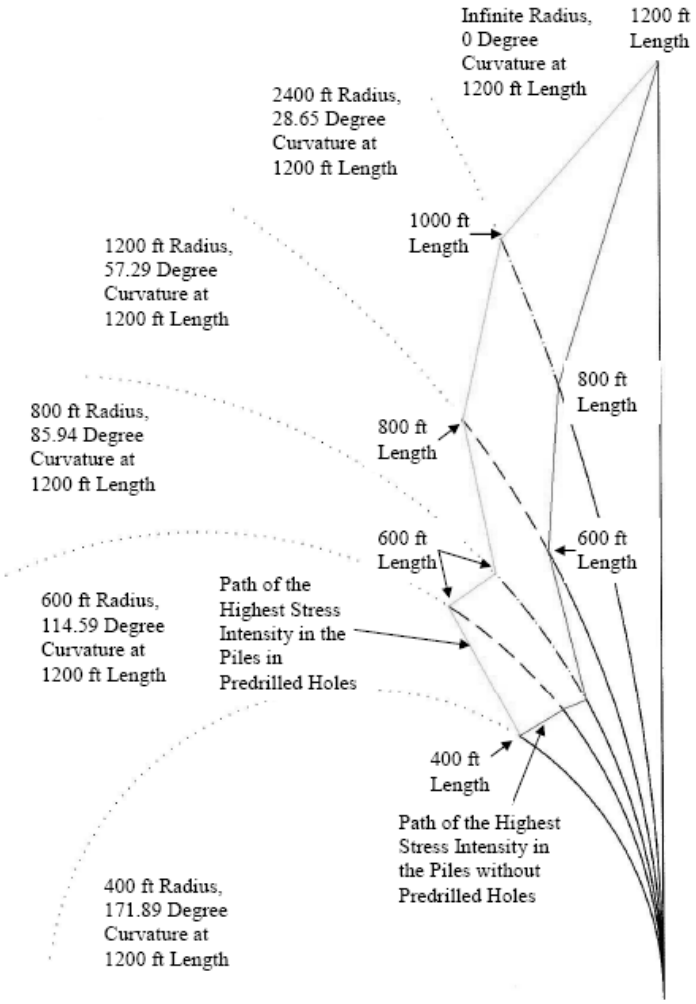

Figure 11. Highest stress intensity in end-bearing piles at different bridge lengths of curved integral abutment bridges of different radii.

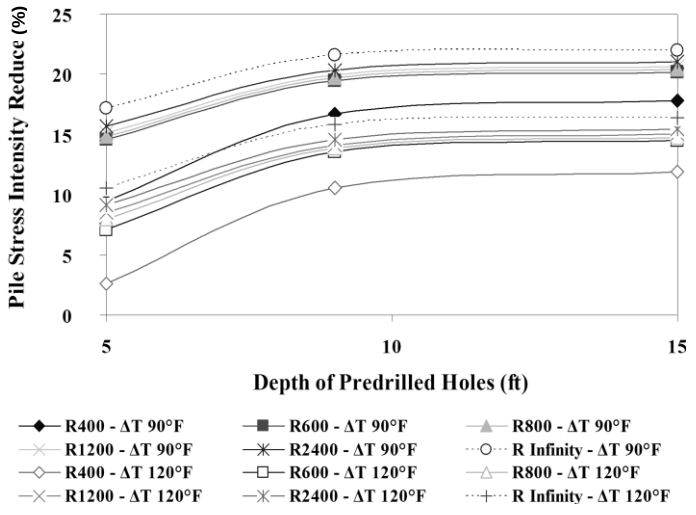

Figure 12. Stress reduction (%) of end-bearing piles in varying depths of predrilled holes of bridges with 30 m (100 ft) spans and bridge length of 30 (100) and 61 m (200 ft).

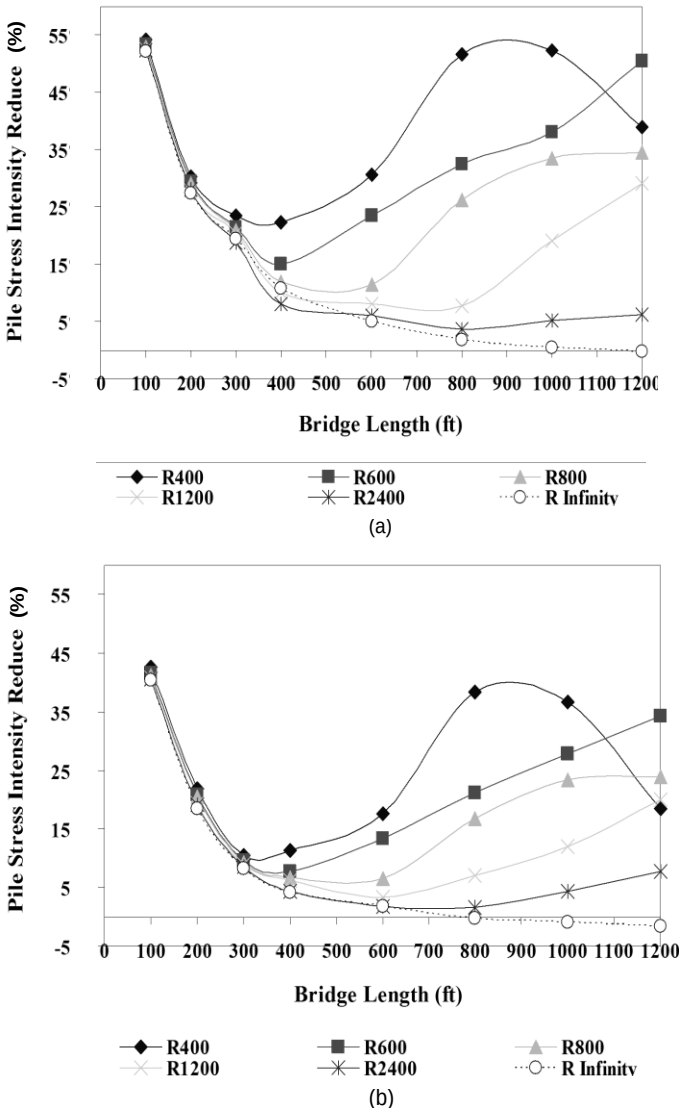

Figure 13. Stress reduction (%) of end-bearing piles in very stiff clay soil profile due to the increase in the number of spans. a) $\Delta T_{slab} = 90° F$, $\Delta T_{the\ rest} = 60° F$; b) $\Delta T_{slab} = 120° F$, $\Delta T_{the\ rest} = 90° F$.

at a shorter bridge length. As the bridge length is increased, the stress intensity in the piles continues to increase until it reaches its highest stress intensity value at a certain bridge length. Beyond that bridge length, it starts decreasing and continues to decrease even though bridge length continues to increase.

(3) Curved IAB's with a smaller radius, for the most part, have a pile stress intensity reduction due to the increase in the number of spans greater than that of curved IAB's with a larger radius.

(4) The pile stress intensity reduction due to the increase in the number of spans of curved IAB's with piles in predrilled holes is greater than that of curved IAB's with piles without predrilled holes. It is shown that piles in 2.7 m (9 ft) deep predrilled holes filled with loose sand have

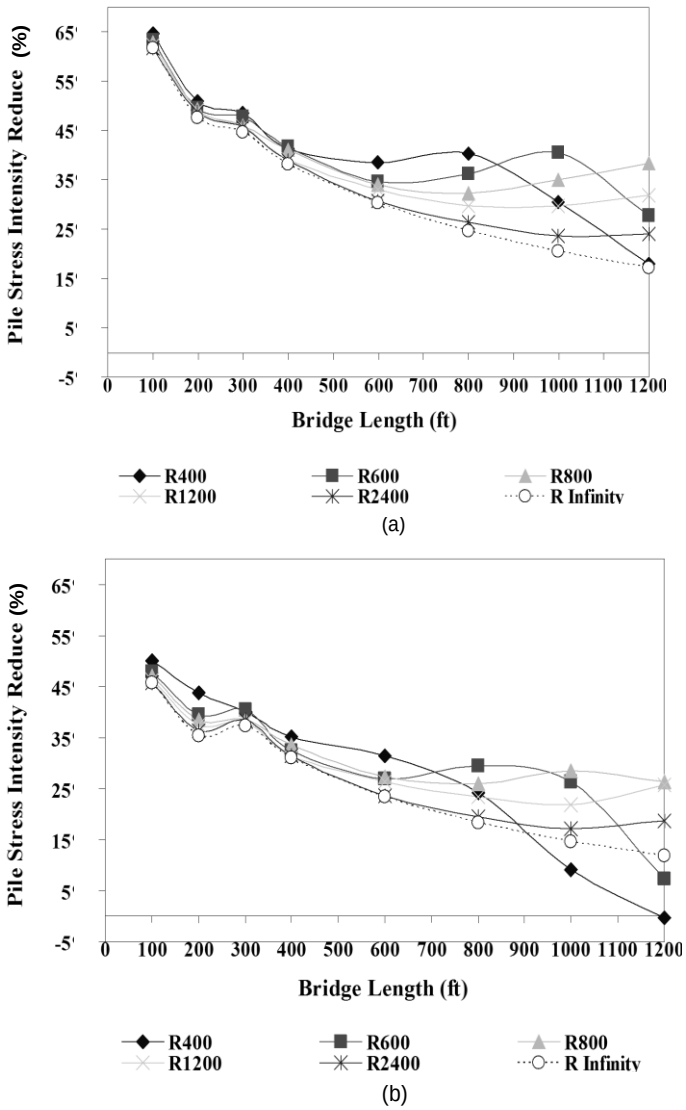

Figure 14. Stress reduction (%) of end-bearing piles in 2.7 m (9 ft) deep predrilled holes due to the increase in the number of spans. a) ΔT_{slab} = 90° F, $\Delta T_{the\ rest}$ = 60° F; b) ΔT_{slab} = 120° F, $\Delta T_{the\ rest}$ = 90° F.

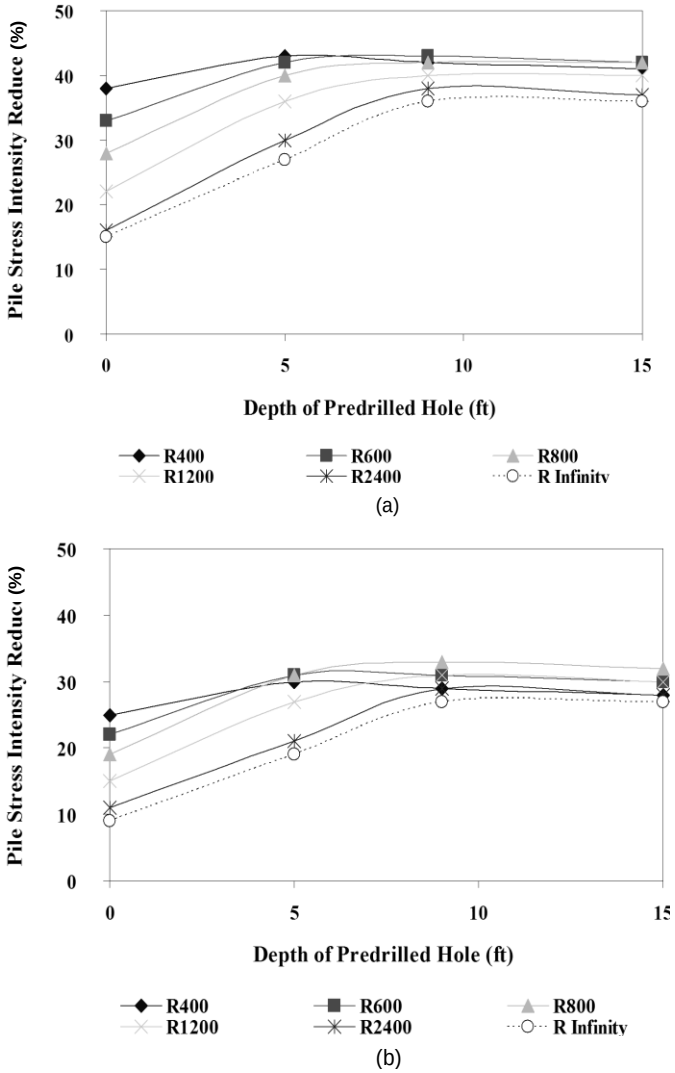

Figure 15. Mean of stress reduction of end-bearing piles in various soil profile types due to the increase in the number of spans. a) ΔT_{slab} = 90° F, $\Delta T_{the\ rest}$ = 60° F; b) ΔT_{slab} = 120° F, $\Delta T_{the\ rest}$ = 90° F.

significantly higher reduction in the pile stress intensity compared to piles in 1.5 m (5 ft) deep predrilled holes filled with loose sand. However, for predrilled holes deeper than 2.7 m (9 ft), the rate of reduction is significantly reduced, which results in only marginal reductions in pile stress intensity.

(5) The difference in pile stress intensity reduction due to the increase in the number of spans between curved IAB's with different radii is smaller when predrilled holes are used for the piles instead of the piles with no predrilled holes.

(6) Increasing the number of spans within a given bridge length results in pile stress reduction. However, this reduction is less at higher temperatures compared to lower temperatures.

Conflict of Interest

The author(s) have not declared any conflict of interests.

REFERENCES

Amde AM, Chini SA, Mafi M (1997). "Experimental study of piles in integral abutment bridges," Int. J. Geotechn. Geol. Eng. 15:343-355. http://dx.doi.org/10.1023/A:1018424027947

Amde AM, Greimann LF, Yang PS (1988). "End bearing piles in jointless bridges," J. Struct. Eng. ASCE. 114(8):1870-1884. http://dx.doi.org/10.1061/(ASCE)0733-9445(1988)114:8(1870)

Amde AM, Klinger J, White EJ (1988). "Performance of jointless bridges," J. Performance Construct. Facilities, ASCE, 2(2):111-125. http://dx.doi.org/10.1061/(ASCE)0887-3828(1988)2:2(111)

Greimann AM, Amde AM, Yang PS (1987). Finite element model for soil-pile interaction in integral abutment bridges. Int. J. Comput. Geotechn, Elsevier Applied Science Publishers Ltd., England, 4:127-149.

Greimann L, Amde AM (1988). "Design Model for Piles in Jointless

Bridges," J. Struct. Eng., ASCE, 114(6):1354-1371.
Greimann LF, Amde AM, Yang PS (1983)."Skewed Bridges with Integral Abutments." Transportation Research Record, No. 903, pp. 64-72.
Greimann LF, Yang PS, Amde AM (1986). "Nonlinear Analysis of Integral Abutment Bridges," J. Struct. Eng. ASCE, 112(10):2263-2280.http://dx.doi.org/10.1061/(ASCE)0733-9445(1986)112:10(2263)
Griton DD, Hawkinson TR, Greimann LF (1991). Validation of design recommendations for integral-abutment piles. J. Struct. Eng. 117(7):2117-2134. http://dx.doi.org/10.1061/(ASCE)0733-9445(1991)117:7(2117)
Haj-Najib R (2002). Integral Abutment Bridges with Skew Angles. PhD thesis. U. of Maryland, College Park. http://dx.doi.org/10.1061/(ASCE)0733-9445(1988)114:6(1354)
Jorgenson JL (1983). Behavior of abutment piles in an integral abutment in response to bridge movements. Transport. Res. Record 903:72-79.
Lawver A, French C, Shield CK (2000). Field performance of integral abutment bridge. Transport. Res. Record 1704:108-117. http://dx.doi.org/10.3141/1740-14
Oesterle RG, Refai TM, Volz JS, Scanlon A, Weiss WJ (2002). Jointless and integral abutment bridges: Analytical research and proposed design procedures. Report FHWA.
Paraschos A, Amde AM (2010). "State of the art and state of design of integral abutment bridges" J. Civil Eng. Practice, Boston Soc. Civil Eng. Section/ASCE, 25(2):35-52.
Yang PS, Amde AM, Greimann LF (1985). "Effects of predrilling and layered soils on piles." J. Geotechn. Eng. ASCE, 111(1):18-31. http://dx.doi.org/10.1061/(ASCE)0733-9410(1985)111:1(18).